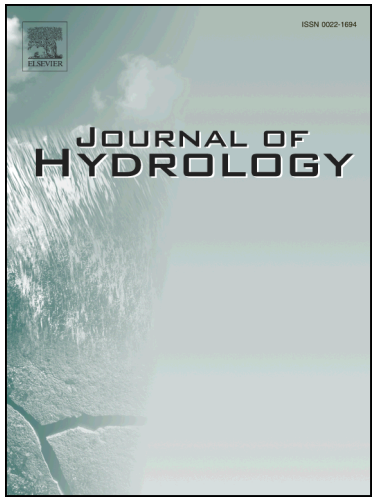

Research papers

Effect of stem cover on hydraulic parameters of overland flow

Hongli Mu, Xianju Yu, Suhua Fu, Bofu Yu, Yingna Liu, Guanghui Zhang

PII: S0022-1694(19)30684-5
DOI: https://doi.org/10.1016/j.jhydrol.2019.123964
Article Number: 123964
Reference: HYDROL 123964

To appear in: *Journal of Hydrology*

Received Date: 9 December 2018
Revised Date: 1 May 2019
Accepted Date: 16 July 2019

Please cite this article as: Mu, H., Yu, X., Fu, S., Yu, B., Liu, Y., Zhang, G., Effect of stem cover on hydraulic parameters of overland flow, *Journal of Hydrology* (2019), doi: https://doi.org/10.1016/j.jhydrol.2019.123964

Effect of stem cover on hydraulic parameters of overland flow

Hongli Mu[a, b], Xianju Yu[a, b], Suhua Fu[a, b, c, *], Bofu Yu[d], Yingna Liu[a, b] and Guanghui Zhang[a, b]

[a]Faculty of Geographical Science, Beijing Normal University, Beijing 100875, PR China.

[b]Beijing Key Laboratory of Environmental Remote Sensing and Digital Cities, Beijing Normal University, Beijing 100875, PR China

[c]State Key Laboratory of Soil Erosion and Dryland Farming on the Loess Plateau, Chinese Academy of Sciences and Ministry of Water Resources, Yangling 712100, PR China

[d]Australian Rivers Institute and School of Engineering and Built Environment, Griffith University, Nathan 4111, Australia

*Corresponding author. E-mail address: suhua@bnu.edu.cn.

Abstract

Vegetation can effectively prevent soil loss and play an important role in soil and water conservation. Accurate estimation of hydraulic parameters is critical for soil erosion models. Hydraulic data for different levels of vegetation stem cover, slope gradient and flow discharge are quite limited. The objectives of this study were to compare different measured methods of flow velocity, to evaluate the influence of vegetation stem cover, slope gradient and discharge on hydraulic parameters and predict the shear stress (τ), stream power (Ω) and unit stream power (ω) and emphasize the significance of hydraulic radius in the calculation of the shear stress (τ), stream power (Ω), and unit stream power (ω). A non-erodible flume bed was used in this study. The discharge ranged from 0.5×10^{-3} to 2.0×10^{-3} m^3 s^{-1}, the slope gradient ranged from 8.8% to 25.9%, and an artificial stem cover of approximately 0, 1.25, 2.5, 5, 10, 15, 20, 25 and 30% was used to represent the natural vegetation. The stems were 2 mm in diameter and randomly arranged. The electrolyte pulse method was preferred for measurement of the overland flow velocity. The flow velocity decreased as the stem cover increased, and flow discharge and slope gradient decreased. The reduction in flow velocity was as high as 90% for 30% stem cover based on the experiments. The flow depth increased as the stem cover and flow discharge increased as the slope gradient decreased. The Reynolds and Froude number values decreased with increasing stem cover. The shear stress, stream power and unit stream power were all significantly affected by the stem cover and could all broadly be described using an exponential delay function of the stem cover. The ω was no significantly impacted by hydraulic radius. Thus, the unit stream power is an improved hydraulic parameter for predicting sediment transport capacity.

Keywords: stem cover; hydraulic parameters; flow discharge; slope gradient; overland flow

1. Introduction

Soil erosion is among the major environmental problems throughout the world (Borrelli, 2013), as it adversely affects agronomic productivity and water quality, particularly in ecologically sensitive regions where the soil resources are fragile, the climate is harsh, and population pressure is high (Lal, 1998). The Loess Plateau of China has suffered from severe soil erosion during the past several decades because of steep terrain, thick erodible soil, sparse vegetation, severe rainstorms, and intense human disturbance (Shi and Shao, 2000; Zhu, 1984; Zhao et al., 2015). In most erosive regions of the Loess Plateau, soil loss is much greater than 25 Mg ha^{-1} a^{-1} (Sun et al., 2013). Vegetation, which is effective in preventing soil erosion, plays an important role in soil and water conservation. Since 1999, the Grain-to-Green Program was implemented on the Loess Plateau of China, and it covered an area of 200×10^4 hectares by 2012. Crops were replaced by trees and grasses in the programme to improve the ecological environment. The hydraulics and soil erosion processes of overland flow have fundamentally changed with extensive re-vegetation on the Loess Plateau. Quantitative research regarding the hydraulic parameters of overland flows could explain and clarify the mechanism of overland flow in relation to soil erosive processes (Ali et al., 2012a; Govers, 1992; Léonard and Richard, 2004), but research on the effect of stem cover on hydraulic parameters on the steep slopes of the Loess Plateau region is limited.

The hydraulic behaviour of a single vegetation element that is completely submerged under the flow surface differs from that which is not submerged (Carollo et al., 2005). Thus, most previous efforts specifically focused on the flow regime, flow velocity, and friction coefficient and their relationships with either submerged or unsubmerged vegetation in the main channels (Carollo et al., 2005; Devi and Kumar, 2016; Dong et al., 2018; Kothyari et al., 2009; Li et al., 2018; Pan and

Shangguan, 2006; Salman et al., 2012; Termini, 2015; Termini, 2016; Turner and Chanmeesri, 1984; Zhang et al., 2017; Zhao et al., 2016). Earlier experimental work on flexible grass-lined channels in a submerged condition was conducted by the United States Department of Agriculture (USDA) Soil Conservation Service (SCS) (1954). Then, experiments in laboratory flumes of submerged vegetation were conducted, e.g., Bao and Li (2017), Carollo et al. (2005), Devi and Kumar (2016), Li et al. (2018), Termini et al. (2016) and Wilson (2007). Large flow depths (> 50 mm), gentle slopes (< 5%), and relatively large flow rates (> 1.5×10^{-3} m^3 s^{-1}) are characteristic of these experiments. These previous investigations focused on different resistance parameters (e.g., Drag or Manning coefficients) and flow velocity in rivers or overland flow. Plants used for these experiments were typically aquatic because the submerged vegetation would grow under the flow surface under natural conditions. Leaf area, stem bending, height and stiffness were used as the main variables. However, the effect of different levels of vegetative cover was not a key parameter for consideration during these experiments.

In addition, the effect of non-submerged vegetation on flow hydraulics has been investigated (Kothyari et al., 2009; Pan and Shangguan, 2006; Salman et al., 2012; Turner and Chanmeesri, 1984; White and Nepf, 2008; Wu and He, 2009; Zhang et al., 2012; Zhang et al., 2018; Zhang et al., 2017; Zhao et al., 2016). Compared to the aforementioned submerged experiment, different levels of vegetative cover, stem diameter and slope steepness and discharge were used as the main variables. Meanwhile, the experimental plants typically were artificial or natural grass with a simple shape. The results of these studies showed that the Reynolds number (*Re*) for vegetated slopes was different from what it was for bare slopes. Zhao et al. (2016) considered that the *Re* for vegetated slopes was much higher than it was for bare slopes, and Pan & Shangguan (2006) and

Wu et al. (2011) found *Re* decreased as vegetative cover increased under simulated rainfall on mobile beds. In addition, the Froude numbers decreased and Manning coefficients increased with increased vegetative cover (Pan and Shangguan, 2006; Salman et al., 2012; Zhao et al., 2016). Flow regime is the basic parameter of hydrodynamic characteristics and directly affects the resistance of overland flow (Roels, 1984). However, flow regime is complex under vegetative cover, and laminar or turbulent and subcritical or supercritical flow cannot be confirmed. The flow velocity is a key determinant of a flow's ability to entrain and carry sediment (Dunkerley, 2003). The velocity decreased with increasing vegetative cover and had a more important effect on flow velocity in the lower section of the slope than in the upper slope section based on measurement in different longitudinal sections (Zhao et al., 2016).

Moreover, some other studies (Guo and Zhang, 2016; Huai et al., 2014) have focused on simulating velocity distributions using models (e.g., the Navier–Stokes–Forchheimer equation) for laminar or turbulent flows through vegetated areas. Meanwhile, based on the experiment results of Termini (2009) and Termini and Piraino (2011) under non-vegetated and vegetated beds, Termini et al. (2016) explored the influence of vegetation on the bed shear stress distribution along the meander wave. They found that the core of the high bed shear stress gradually shifts outward at the bend entrance and maintains higher values near the outer bank under a non-vegetated bed. The introduction of vegetation leads to high friction coefficients and low bed shear stresses particularly in the outer-bank region. White and Nepf (2008) accurately predicted the shear stress of the vegetation interface by focusing on the dynamics of the coherent structures. Meanwhile, White and Nepf (2008) thought that their study was not only essential in predicting velocity distribution but also was important for studies of sediment transport. Hydraulic parameters (e.g., flow velocity,

shear stress, stream power and unit stream power) have been typically used to predict sediment transport capacity in many studies (Abrahams et al., 2001; Ali et al., 2012a; Govers, 1990; Li and Abrahams, 1999; Mahmoodabadi et al., 2014; Zhang et al., 2009). However, few studies have examined the effect of different vegetative stem covers on shear stress (τ), stream power (Ω), and unit stream power (ω) and predicted the τ, Ω and ω using the stem cover, slope and discharge.

The vegetative cover of traditional studies considered the combined role of leaves and stems. However, vegetative stems behave as the dominant roughness element in overland flow (Zhao et al., 2016). Thus, the objectives of this study were to (1) to compare different measured methods of flow velocity; (2) quantify the effect of vegetative stem cover on the hydraulic parameters of overland flows for a range of discharge and slope steepness values; (3) predict the shear stress (τ), stream power (Ω) and unit stream power (ω) and emphasize the significance of hydraulic radius in the calculation of the shear stress (τ), stream power (Ω), and unit stream power (ω). The results are helpful for simplifying the calculation of hydraulic parameters to predict sediment transport capacity to better understand the mechanism underlying the role of vegetative stems in soil and water conservation.

2. Materials and Methods

2.1 Experimental conditions and treatments

This study was conducted at the Fangshan experimental station of Beijing Normal University. The experiments on hydraulic parameters of overland flows were conducted in a flume (5.0 m in length and 0.37 m in width) with a smooth Plexi-glass floor and glass walls (Fig. 1a). The bed slope of the flume could be manually adjusted from 0 to 60%. The flume consisted of a 2.4-m-long section covered with artificial vegetative stems and a 2.3-m-long bare section with a layer of

sieved sediment; the top 0.3 m was the head tank (Fig. 1b). To simulate the effect of vegetative stems on the hydraulic parameters of overland flows, Gramineae stems were chosen to ensure that the they could protrude through the overland flow. The Gramineae stems were 2 mm in diameter and 12 cm in height. The stems were artificial and had similar flexibility to that of natural vegetative stems. Moreover, the Gramineae stems could be reused. The basal cover and layout of the Gramineae stems can be more easily controlled than those of a natural vegetative stem. According to the typical vegetation cover on the Loess Plateau, the stem cover values assessed in this study were approximately 0, 1.25, 2.5, 5, 10, 15, 20, 25 and 30%, and they were controlled by the total number of stems and stem diameter; details are provided in Table 2 of Mu et al. (2019). For each level of stem cover, a plastic mesh with punched holes was used to secure the artificial Gramineae stems and then placed on the flume bed covered with oil paint. A thick layer of sieved sand was added into the paint to increase the bed roughness. The stems were glued to the flume bed when the paint was dry, and the bed material for areas not covered with stems was the same as that used for the experiment to measure the hydraulic parameters on bare surfaces. The stems were arranged in a random pattern (Fig. 2a), and a stem cover of 30% resulted in a nearly 100% canopy cover (Fig. 2b). The bare 'ground' between the stems (70%) could not be seen from above the artificial stems because the artificial Gramineae stems are sufficiently flexible to conceal the bare ground surface for a closed canopy.

The sediment, which was collected from the bed of the Yongding River near Beijing, was air dried and first passed through a 2-mm sieve to remove gravel and residues. The sand that passed through a 0.59-mm sieve but not a 0.25-mm sieve was used as the experimental material; the median diameter (d_{50}) was 0.35 mm. The experimental flume was adjusted to 8.7, 17.4 and 25.9%,

corresponding to common slope gradients found in the Loess Plateau region. Three discharges were used, i.e., 0.5×10^{-3}, 1.0×10^{-3} and 2.0×10^{-3} m^3 s^{-1}. These correspond to overland flow from areas 4 m in width and 9 to 36 m in length with a steady state rainfall intensity of 50 mm hr^{-1} to contextualize the magnitude of the discharge applied. The discharge was controlled by a series of valves installed in a flow diversion box. The discharge was collected at the lower end of the flume using plastic buckets and measured using a volumetric cylinder.

2.2 Experimental measurements

The flow discharge, slope gradient, and stem cover were adjusted to designated values before flow introduction. After the flow stabilized, the flow depth was measured using three level probes (SX40-A, Chongqing Hydrological Equipment Factory) across three sections (Fig. 3a) located at 0.3, 0.6 and 0.9 m above the lower end of the flume (Fig. 1b). The resolution of the level probe was 0.1 mm, and the accuracy was 0.3 mm. In total, 12 depths were measured at each cross section. The maximum and minimum flow depths were eliminated from the observed values for each section. The remaining 10 measured values were averaged for each cross section. At last, the flow depth was the average of the three cross sections.

The mean flow velocity was measured using two methods. One was the electrolyte pulse method of shallow flow (QYLS-303, Xian Qingyuan Measurement and Control Technology Co., LTD) (Lei et al., 2010). The measurement system included four parts: a salt solute injector (Fig. 3b) located at 3.0 m from the lower end of the flume (Fig. 1b); six electric conductivity sensors (Fig. 3c) located at 0.2, 0.7, 1.2, 1.7, 2.2, and 2.7 m above the lower end of the flume (Fig. 1b); an interface unit (Fig. 3d) connecting the salt solute injector, electric conductivity sensors and computer; and last, a computer installed with specially designed software (Fig. 3d) (Lei et al.,

2010). The procedures were typically as follows (Lei et al., 2010): (1) when the flow stabilized, the computer initiated data logging and a highly saturated salt solute of *KCL* was injected into the flow via the salt solute injector. (2) Sufficient time was allowed for the solute to transport and pass through each sensor. (3) The electric conductivity sensor values as a function of time were recorded by the specially designed software. (4) Data logging was stopped. (5) The analysis part of the software was run to fit the logged data and estimate the velocities at different locations. (6) Computed velocity values were outputted.

The measurement system was an automated data collection and processing system and velocities were estimated at different longitudinal sections. There were three replicates for each combination of flow discharge, slope gradient, and stem cover. The sensors were 2.7 m and 2.2 m above the lower end of the flume and were outside of the stem cover; thus, the measured results of the two sensors were ignored during this study. The other velocities of the four sensors were impacted by stem cover. With an increase in stem cover, there were some differences between the velocity measurements based on sensors that were 1.7 m and 0.2 m above the lower end of the flume (Sensors 1 and 4) (Fig. 4a, Table 1), but the velocity values of last two sensors (Sensors 3 and 4) were quite consistent (Fig. 4b, Table 1). Thus, the velocity values based on Sensors 3 and 4 were averaged for each replicate. Then, the average of the three replicates was used as the mean flow velocity (V_{pul}) (Table 2).

The second method was based on $KMnO_4$ tracing. A small amount of dye was quickly injected into the flow using a dropper with a rubber head. The travel time of the leading edge of the dye cloud was measured over a distance of 2 m along the flume using a digital stopwatch. The leading edge of the dye cloud was visually observed, which may have caused some errors in travel time

measurements (Dunkerley, 2001). When travel times were measured and found to be too long or too short, the measurement was discarded and repeated. The dye-based flow velocity (V_{dye}) was estimated by dividing the length along the flume (2 m) by the measured travelling time of the dye cloud. To compare the two different methods of flow velocity measurements, the dye-based flow velocity measurements were taken at the same locations of 2.2 m and 0.2 m above the lower end of the flume. Twelve dye-based velocity measurements were taken across one section. The maximum and minimum measured flow velocities were eliminated from each section and the mean of the remaining 10 velocities was considered as the mean velocity for that section (Table 2). Then, this value was multiplied by a correction factor (α) at different laminar (α=0.67), transitional (α=0.7) and turbulent (α=0.8) flows (Dunkerley, 2001; Horton et al., 1934; Li et al., 1996; Zhang et al., 2010).

2.3 Data Analysis

Vegetative stem cover was calculated using the stem diameter, the number of stems, and the size of the flume bed as follows:

$$C = \frac{N\pi D^2}{4WL} \tag{1}$$

where C is the fractional vegetative stem cover (-), N is the total number of stems over the flume area, D is the stem diameter (m), W is the flume width (0.37 m), and L is the vegetated length (2.4 m).

The effective flow width did not equal the flume width because of the protuberant obstacles, which could be calculated as follows (Abrahams et al., 2001):

$$w = W \times (1 - C) \tag{2}$$

where w is the effective flow width (m). The effect of the vegetative stems on the unit flow

discharge was considered. The unit flow discharge was then calculated by dividing the flow discharge by w:

$$q = Q / w \tag{3}$$

where q is the unit discharge ($m^2\ s^{-1}$) Q is the discharge ($m^3\ s^{-1}$). The hydraulic radius (R) was defined as the ratio of the cross-sectional area to the wet perimeter as follows:

$$R = A / P \tag{4}$$

and the cross-sectional area A (m^2) and wet perimeter P (m) were calculated, respectively, as follows:

$$A = w \times H \tag{5}$$

$$P = \frac{2HL + \left(WL - \frac{N\pi D^2}{4} \right) + \pi DHN}{L} \tag{6}$$

where H is the flow depth (m). The mean inter-stem velocity was estimated as follows:

$$V_{dep} = Q / (H \times w) \tag{7}$$

where V_{dep} is the mean velocity calculated based on the continuity equation. Based on a comparison of different velocity measurements (see Section 3.1 below), all hydraulic parameters were calculated using V_{pul} for this study.

The Reynolds number is a dimensionless number and is often used to characterize different flow regimes, such as laminar or turbulent flows. The Reynolds number (Re) was calculated as follows:

$$Re = RV_{pul} / v_m \tag{8}$$

where V_{pul} is the mean velocity measured using the electrolyte pulse method ($m\ s^{-1}$) and v_m is the kinematic viscosity.

The Froude number is defined as the ratio of inertia to gravitational forces, reflecting the interaction between the flow depth and velocity. Subcritical flow occurs when Fr<1, and supercritical flow occurs when Fr>1. The Froude number (Fr) was expressed as follows:

$$Fr = V_{pul} / \sqrt{gH} \tag{9}$$

where g is the gravitational acceleration (m s^{-2}).

Among the most frequently used variables is the shear stress of shallow flow based on the bed load formula of Yalin (1963), as follows:

$$\tau = \rho \mathrm{gRS} \tag{10}$$

where τ is the shear stress (Pa), ρ is the water density (kg m^{-3}), and S is the sine bed slope (m m^{-1}). The stream power concept was introduced by Bagnold (1966) who assumed that the sediment transport rate was a function of the time rate of potential energy expenditure per unit bed area as follows:

$$\Omega = \tau V_{pul} \tag{11}$$

where Ω is the stream power (kg s^{-3}). Yang (1972) assumed that the sediment transport rate was a function of the time rate of potential energy expenditure per unit weight of water as follows:

$$\omega = V_{pul} S \tag{12}$$

where ω is the unit stream power (m s^{-1}).

The following statistical parameters were used to evaluate the performance of the flow velocity and stream power equations:

i) Relative root of the mean squared error (*RRMSE*):

$$RRMSE = \frac{\sqrt{(1/n)\sum_{i=1}^{n}(O_i - P_i)^2}}{O_m} \quad (13)$$

where O_i are the observed values. P_i are the predicted values, and O_m is the mean of the observed values.

ii) Coefficient of Nash–Sutcliffe model efficiency (*NSE*):

$$NSE = \frac{\sum_{i=1}^{n}(O_i - O_m)^2 - \sum_{i=1}^{n}(P_i - O_i)^2}{\sum_{i=1}^{n}(O_i - O_m)^2} \quad (14)$$

iii) Coefficient of determination (R^2):

$$R^2 = \frac{\left[\sum_{i=1}^{n}(O_i - O_m)(P_i - P_m)\right]^2}{\sum_{i=1}^{n}(O_i - O_m)^2 \sum_{i=1}^{n}(P_i - P_m)^2} \quad (15)$$

where P_m is the mean of the predicted value.

Relationships between the slope gradient, unit flow discharge, and stem cover and shear stress, stream power and unit stream power were analysed using nonlinear regression models. The influence of slope gradient, discharge, and stem cover on the V, H, Re, Fr, τ, Ω and ω was analysed via *ANOVA*. All analyses were conducted using the Statistical Product and Service Solutions (*SPSS*) software (version 20.0) at the 0.05 significance level.

3. Results

3.1 *Comparison of different velocity measurement methods*

Conductivity probe and $KMnO_4$ tracing methods are frequently used for measurements of the flow depth and velocity (Ali et al., 2012b; Pan and Shangguan, 2006; Wu, 2011; Zhang et al., 2017). Thus, the V_{pul} (using the electrolyte pulse method) was compared to the V_{dye} (using the $KMnO_4$ tracing method) and the V_{dep} (determined using the continuity equation and measured flow depth). The *MAE* and *RRMSE* between the V_{pul} and V_{dep} and between the V_{pul} and V_{dye} were

less than those between the V_{dye} and V_{dep}. The *NSE* between the V_{pul} and V_{dep} and between the V_{pul} and V_{dye} were greater than those between the V_{dye} and V_{dep} (Table 3). In addition, significant linear relationships were found between the V_{pul} and V_{dye} and the V_{pul} and V_{dep} based on regression analysis. The R^2 of both equations was 0.98 (Fig. 5). Moreover, there were some differences among the three velocities. The V_{pul} was slightly higher than the V_{dep} (Fig. 5a) and was slightly less than the V_{dye} for the bare cover (Fig. 5b); the V_{pul} was slightly higher than the V_{dep} and V_{dye} for the stem cover (Fig. 5). The reason may be that the relative error in the flow depth measurement increased with increasing slope and decreasing discharge. The $KMnO_4$ tracing method was affected by turbulent and supercritical flows and the error in the measured velocity increased as the velocity increased. The measurement of flow depth and V_{dye} was not only impacted by hydrodynamic force, but also obstructed as the stem cover increased. In addition, it took 40 min to measure the flow depth but 20 min for V_{dye}. The electrolyte pulse method only used 3 min and was much less affected by human factors; it was more objective. Thus, the electrolyte pulse method for measuring the overland flow velocity of the stem cover is highly recommended. The V_{pul} was used as the measured flow velocity for this study.

3.2 Flow velocity and flow depth

The flow velocity was measured using the electrolyte pulse method (Lei et al., 2010) at four longitudinal sections (Table 1). There were no significant differences in flow velocity among the four longitudinal sections (P>0.05). However, the velocity at the most downstream section (Sensor 4) was slightly higher than that of the upstream section (Sensor 1) when there was no stem cover, and it was slightly lower than that of the upstream section (Sensor 1) when there was stem cover (Fig. 4a). The measured velocities of Sensor 3 were quite consistent with those of Sensor 4

for all conditions (Fig. 4b). Thus, the mean flow velocity, V_{pul}, was based on measurements recorded using Sensors 3 and 4 because of the spatial consistency (Fig. 4b).

The mean velocity on the bare flume ranged from 0.422 to 0.951 m s^{-1} and that with stem cover from 0.063 to 0.502 m s^{-1} (Fig. 6, Table 2). The mean velocity decreased as the stem cover increased, and it increased as the flow discharge and slope gradient increases (Fig. 6). The V_{pul} was significantly affected by the stem cover, slope and discharge (P<0.01). Compared to the bare flume under different slopes and discharges, the stem cover of 1.25% reduced the flow velocity by a factor of 0.48-0.56 and the stem cover of 30% reduced the flow velocity by a factor of 0.09-0.18 (Table 4). Thus, the reduction in flow velocity can be as high as 90% for 30% stem cover. The flow depth (H) ranged from 3.35 to 8.28 mm on the bare flume and from 5.50 to 82.8 mm with stem cover. H increased as the stem cover and discharge increased and slope gradient decreased (Fig. 7). H was significantly affected by stem cover and discharge (P<0.01). H/H_o, where H_o is the flow depth without stem cover, varied between 1.64 and 2.05 when the stem cover was 1.25%; the ratio increased to 4.67-10.0 for a stem cover of 30% (Table 4).

3. 3 Flow regime

The Reynolds number (Re) ranged from 86 to 7667 (Fig. 8). The overland flows were laminar when the stem cover was between 15% and 30%, transitional when the stem cover was between 2.5% and 10%, and turbulent when the stem cover was ≤ 2.5%. Thus, the Re was significantly impacted by the stem cover (P<0.01). The Re decreased with an increase in the stem cover. Pan & Shangguan (2006) and Wu et al. (2011) also found that Re decreases as the vegetation cover increases under simulated rainfall on mobile beds. However, Zhao et al. (2016) thought that the Re

with stem cover was higher than that from a bare flume because the stem cover could decrease the effective flow width and increase the unit flow discharge.

The Froude number (*Fr*) ranged from 0.07 to 3.98 (Fig. 9). The overland flows were supercritical when the stem cover was between 0 and 2.5% and subcritical when the stem cover was greater than 2.5%. This result was consistent with that provided by Hashimoto (2007) who found that the overland flow frequently encountered supercritical flows on vegetated steep slopes. There were significant differences in the *Fr* under different stem covers and slopes ($P<0.01$), but there was not an obvious discrepancy under different discharges ($P>0.05$). The stem cover of 1.25% led to a decrease of approximately 63% in the *Fr* compared to that of the bare flume. The decrease in *Fr* with stem cover shows that vegetation stems could decrease the stream power and the ability of runoff to carry sediment (Pan and Shangguan, 2006; Wu et al., 2011).

3. 4 Shear stress, stream power and unit stream power

The shear stress (τ), stream power (Ω), and unit stream power (ω) ranged from 1.11 to 21.84 Pa, from 0.07 to 13.66 kg s^{-3}, and from 0.01 to 0.25 m s^{-1}, respectively (Fig. 10). The τ reached its peak when the stem cover was 1.25% and then decreased as the stem cover increased (Fig. 10a). The trend of Ω and ω with stem cover were different from that of the τ. The Ω and ω decreased as the stem cover increased (Fig. 10b, c). The different trend with stem cover may have been caused by the hydraulic radius. The hydraulic radius followed the same trend as that of τ; the maximum value appeared at a stem cover of 1.25%. The τ was significantly affected by the hydraulic radius ($P<0.01$) (Fig. 11). The Ω was more affected by the flow velocity ($P<0.01$) than by the hydraulic radius ($P<0.05$). The ω was significantly impacted by flow velocity ($P<0.01$). Thus, the trend of Ω and ω with stem cover was similar to that of the flow velocity. Compared to the bare flume for

different slopes and discharges, the corresponding decreasing rate of τ, Ω and ω for different stem covers was different. The τ increased by a factor of 1.32-1.63 for 1.25% stem cover and decreased by a factor of 0.17-0.38 for 30% stem cover (Fig. 12, Table 4). The Ω decreased by a factor of 0.63-0.87 for 1.25% stem cover and by a factor of 0.02-0.07 for 30% stem cover (Fig. 12, Table 4). The ω decreased by a factor of 0.48-0.56 for 1.25% stem cover and by a factor of 0.09-0.18 for 30% stem cover (Fig. 12, Table 4).

Nonlinear regression analysis was conducted based on the unit discharge and slope gradient when there was no stem cover. The equations (Eqs. [16]-[18]) for estimating the τ, Ω and ω were obtained (Table 5). *NSE* and R^2 for the three equations were 0.99. Table 5 shows that the slope exponents of Eqs. [16]-[18] were greater than those of the unit flow discharge, showing that the slope gradient played a more important role in increasing the flow energy for the bare flume. Based on Eqs. [16]-[18], the effect of stem cover on τ, Ω and ω was considered. New regression equations were developed. The *NSE* values of Eq. [19], Eq. [20] and Eq. [21] were 0.73, 0.98 and 0.71, respectively. The corresponding R^2 values were 0.84, 0.98 and 0.84, respectively (Table 5). The stream power (Ω) was better predicted by the slope gradient, unit discharge and stem cover than the τ and ω in this study.

4. Discussion

4.1 Comparison of the flow velocity under vegetation cover

The mean velocity of stem cover varied from 10% to 30% in this study and was near that of 50% vegetation cover in simulated rainfall experiments (Zhang et al., 2012). However, compared to the bare flume, the stem cover varying from 10% to 30% reduced the flow velocity by a factor of 0.09-0.33 for different slopes and discharges (Table 4). A vegetation cover of 50% in Zhang et al.,

(2012) reduced the flow velocity by a factor of 0.56 for different rainfall intensities. The reduction factor for 50% vegetation cover from Zhang et al. (2012) was greater than that from the stem cover ranging from 10% to 30% in this study and was similar to the stem cover of 1.25% (Table 4). In addition, Pan and Shangguan (2006) reported that a vegetation cover varying from 35% to 90% decreased the flow velocity by a factor of 0.40-0.55 for different rainfall intensities. The reduction factor of Pan and Shangguan (2006) was also similar to the stem cover varying from 1.25% to 5% in this study. These results show that the stem cover had a greater effect on the flow velocity than the vegetation cover. The differences in the reduction factor may have been caused by the manner in which the cover was defined. The vegetation cover was used in Pan and Shangguan (2006) and Zhang et al. (2012), while stem cover was used in this study. The vegetation cover is generally greater than the stem cover when the stem density and diameter remain constant. Thus, the stem cover provide higher surface roughness than that of the vegetation cover under the same cover percentage, resulting in a greater decrease in the flow velocity. Except for the effect of cover, the experiments of Pan and Shangguan (2006) and Zhang et al. (2012) were an erodible bed with soil and a non-erodible bed with uniform sand was used in this study, which may have caused the difference in decreasing flow velocity.

4.2 *Performance of equations for shear stress, stream power and unit stream power*

The experimental data from Pan and Shangguan (2006), Zhang et al. (2011), and Zhao et al. (2016) were used to test the accuracy of the equations developed in this study. These data were selected because of the similar experimental conditions or similar vegetation. The experiment of Pan and Shangguan (2006) used natural grass, and the diameter and stiffness were similar to those of this study. This experiment used the same method and equipment as the study of Zhang et al.

(2011). The experimental condition of Zhao et al. (2016) and this study used a non-erodible bed and overland flow. More importantly, the cover of Zhao et al. (2016) was also stem cover because *PVC* cylinders served as vegetation stems. Thus, Eq. [16]-[18] showed good accuracy for predicting τ, Ω and ω under the study of Zhang et al. (2011). The *RRMSE* values for Eqs. [16], [17] and [18] were 0.31, 0.14, 0.18, respectively; the corresponding *NSE* were 0.50, 0.96 and 0.90 and the R^2 were 0.99, 0.98 and 0.98, respectively (Table 6).

To test the performance of Eqs. [19]-[21], the τ, Ω and ω values from Pan and Shangguan (2006) and Zhao et al. (2016) were predicted and compared. Eqs. [19]-[21] provided the high R^2 values and poor *RRMSE* and *NSE* values from the experimental data of Pan and Shangguan (2006) (Table 6). This finding implies that the τ, Ω and ω of Pan and Shangguan (2006) could not be predicted using Eqs. [19]-[21] of this study. The possible reasons were as follows. First, Pan and Shangguan (2006) used the flow depth as the hydraulic radius to calculate the hydraulic parameters because they did not record the amount of vegetation at different covers and the hydraulic radius could not be calculated. Although many studies (Abrahams et al., 2001; Ali et al., 2012a; Pan and Shangguan, 2006; Zhang et al., 2009; Zhao et al., 2016) found that the hydraulic radius could be replaced by the flow depth, the hydraulic radius was significantly different with flow depth under the vegetative stem cover in this study (P<0.05) (Fig. 7, 11). Therefore, the hydraulic radius could not be replaced by the flow depth particularly when the vegetative stem diameter was small. Second, simulated rainfall was used in the experiments of Pan and Shangguan (2006). The flow discharge was less than that from this study (Table 6).

Compared to the τ and Ω values of Zhao et al. (2016) and predicted values from Eqs. [19]-[20], the *RRMSE* values of Eqs. [19]-[20] were 0.55 and 0.60, the corresponding *NSE* values were -2.69

and -1.65, and the R^2 values were 0.07 and 0.39, respectively (Table 6). This finding implies that the τ and Ω of Zhao et al. (2016) could not be predicted using Eqs. [19]-[20]. The possible reasons were three aspects. First, the cylinder diameters (20, 32 and 40 mm) of Zhao et al. (2016) were much larger than those used in this study (2 mm). The hydraulic radius was significantly impacted by vegetation diameter (P<0.01). This discrepancy was caused by the hydraulic radius, which resulted in a trend and magnitude of the τ and Ω with the stem cover in this study being different from those provided by Zhao et al. (2016). The τ of Zhao et al. (2016) increased as the stem cover increased (Fig. 13a), and the Ω of Zhao et al. (2016) decreased as the stem cover increased (Fig. 13b). In addition, the magnitudes of τ and Ω from Zhao et al. (2016) were greater than those from this study when the stem cover was greater than 10% (Fig. 13a, b). Second, the artificial Gramineae stems of this study were flexible, and the *PVC* cylinders of Zhao et al. (2016) were very stiff, which resulted in a different roughness at a similar discharge and slope gradient. Third, silt-laden flow was used during the experiment of Zhao et al. (2016) but no silt-laden flow was used in this study.

Notably, Eq. [21] provided a better estimation for the ω compared to that from Zhao et al. (2016). The *RRMSE* of Eq. [21] was 0.33, the corresponding *NSE* was 0.48, and the R^2 was 0.90 (Table 6). The magnitude of the unit stream power was quite near that in this study with the same stem cover (Fig. 13c). Thus, the performance of Eq. [21] was better than that of Eq. [19] and Eq. [20]. The possible reason was that ω was not significantly impacted by the hydraulic radius. In addition, Zhao et al. (2016) had a similar slope gradient and flow discharge to that in this study. The τ, Ω and ω are typically used to predict sediment transport capacity in many studies (Abrahams et al., 2001; Ali et al., 2012a; Govers, 1990; Li and Abrahams, 1999; Mahmoodabadi

et al., 2014; Zhang et al., 2009). The results from this study show that ω was the better hydraulic parameter to predict sediment transport capacity. Gimenez and Govers (2002) also believed that ω could reflect the surface roughness better than τ and Ω.

5. Conclusions

For overland flows with a discharge ranging from 0.5 to 2 L/s and a slope from 8.8% to 25.9%, a number of hydraulic parameters were measured with a vegetative stem cover of up to 30% to investigate the effect of cover on overland flow hydraulics. The following conclusions can be drawn based on this experimental study:

- The electrolyte pulse method is preferred for measurement of overland flow velocity because it is efficient and objective.
- Flow velocity is positively correlated with discharge and slope steepness, and negatively related to stem cover, as expected. Based on this set of experiments, the reduction in flow velocity can be as high as 90% for 30% stem cover.
- Flow depth increased when stem cover and flow discharge increased and the slope gradient decreased. The flow depth was significantly impacted by stem cover and flow discharge (P<0.01). A stem cover of 1.25% showed ratios of approximately 1.64-2.05 in flow depth compared to that of the bare flume under different slopes and discharges and a stem cover of 30% which showed ratios of approximately 4.67-10.00.
- Both the Reynolds (*Re*) and Froude (*Fr*) numbers decreased with stem cover. For this set of experiments, based on *Re* and *Fr*, hydraulic parameters were measured for both laminar and turbulent and both subcritical and supercritical flows.
- While the shear stress, stream power and unit stream power were all significantly affected

by the stem cover, they could all broadly be described using an exponential delay function of cover. There were subtle differences in the manner in which these hydraulic parameters were related to discharge, slope and cover: 1) the shear stress showed a local maximum at a stem cover of 1.25%. 2) The Ω and ω decreased as the stem cover increased. The τ was significantly affected by the hydraulic radius. The Ω was more affected by the flow velocity than by the hydraulic radius. The ω was no significantly impacted by hydraulic radius. The unit stream power was the best hydraulic parameter to predict sediment transport capacity.

Acknowledgements

This research was funded by the State Key Program of the National Natural Science Foundation of China (No. 41530858), the National Natural Science Foundation of China (No. 41571259), the CAS "Light of West China" programme, the programme for Changjiang Scholars and Innovative Research Team in University and the China Scholarship Council.

REFERENCES

Abrahams, A.D., Li, G., Krishnan, C., Atkinson, J.F., 2001. A sediment transport equation for interrill overland flow on rough surfaces. Earth Surf. Process. Landf. 26(13), 1443-1459.

Ali, M., Sterk, G., Seeger, M., Boersema, M., Peters, P., 2012a. Effect of hydraulic parameters on sediment transport capacity in overland flow over erodible beds. Hydrol. Earth Syst. Sci. 8(4), 6939-6965.

Ali, M., Sterk, G., Seeger, M., Stroosnijder, L., 2012b. Effect of flow discharge and median grain size on mean flow velocity under overland flow. J. Hydrol. 452, 150-160.

Bagnold, R.A., 1966. An approach to the sediment transport problem from general physics. US Geol. Surv. Prof. Pap., 422-I, 37.

Bao, M.X., Li, C.W., 2017. Hydrodynamics and bed stability of open channel flows with submerged foliaged plants. Environ. Fluid Mech.17(4), 815-831.

Borrelli, P., 2013. Modelling post-tree-harvesting soil erosion and sediment deposition potential in the Turano River Basin (Italian Central Apennine). Land Degrad. Dev. 26(4), 356-366.

Carollo, F., Ferro, V., Termini, D., 2005. Flow resistance law in channels with flexible submerged vegetation. J. Hydrol. Eng. 131(7), 554-564.

Devi, T.B., Kumar, B., 2016. Experimentation on submerged flow over flexible vegetation patches with downward seepage. Ecol. Eng. 91, 158-168.

Dong, Y.F., Xiong, D.H., Su, Z.A., Yang, D., Zheng, X.Y., Shi, L.T., Poesen, J., 2018. Effects of vegetation buffer strips on concentrated flow hydraulics and gully bed erosion based on in situ scouring experiments. Land Degrad. Dev. 29(6), 1672-1682.

Dunkerley, D., 2001. Estimating the mean speed of laminar overland flow using dye injection-uncertainty on rough surfaces. Earth Surf. Process. Landf. 26(4), 363–374.

Dunkerley, D.L., 2003. An optical tachometer for short path measurement of flow speeds in shallow overland flows: improved alternative to dye timing. Earth Surf. Process. Landf. 28(28), 777-786.

Giménez, R., Govers, G., 2002. Flow detachment by concentrated flow on smooth and irregular beds. Soil Sci. Soc. Am. J. 66(5), 1475-1483.

Govers, G., 1990. Empirical relationships for the transport capacity of overland flow. Erosion, Transport, and Deposition Processes, Proceedings of Jerusalem Workshop. Jerusalem,

Israel, pp. 45-63.

Govers, G., Parsons, A.J., Abrahams, A.D., 1992. Evaluation of transporting capacity formulae for overland flow conditions, in: Parsons, A.J., Abrahams, A.D. (Eds.), Overland Flow Hydraulics and Erosion Mechanics. University College London Press, London, PP.

Guo, J., Zhang, J., 2016. Velocity distributions in laminar and turbulent vegetated flows. J. Hydraul. Res. 54(2), 117-130.

Hashimoto, H., Park, K., Nagabayashi, H., Hayashi, K., 2007. Bed fluctuation in an open channel with riparian trees. In Proc. 10th Intl. Symp. River Sedimentation, Moscow, 118–126.

Hooke, J., 2003. Coarse sediment connectivity in river channel systems: a conceptual framework and methodology. Geomorphology 56(1), 79-94.

Horton, R.E., Leach, H.R., Vliet, R.V., 1934. Laminar sheet-flow. Eos, Trans. Am. Geophys. Union 15(2), 393-404.

Huai, W., Wang, W., Hu, Y., Zeng, Y., Yang, Z., 2014. Analytical model of the mean velocity distribution in an open channel with double-layered rigid vegetation. Adv. Water Resour. 69, 106-113.

Järvelä, J., 2002. Flow resistance of flexible and stiff vegetation: a flume study with natural plants. J. Hydrol. 269(1), 44-54.

Kothyari, U.C., Hayashi, K., Hashimoto, H., 2009. Drag coefficient of unsubmerged rigid vegetation stems in open channel flows. J. Hydraul. Res. 47(6), 691-699.

Lal, R., 1998. Soil erosion impact on agronomic productivity and environment quality. Crit. Rev. Plant Sci. 17(4), 319-464.

Lei, T.W., Chuo, R.Y., Zhao, J., Shi, X.N., Liu, L., 2010. An improved method for shallow water

flow velocity measurement with practical electrolyte inputs. J. Hydrol. 390, 45-56.

Léonard, J., Richard, G., 2004. Estimation of runoff critical shear stress for soil erosion from soil shear strength. Catena 57(3), 233-249.

Li, G., Abrahams, A.D., 1999. Controls of sediment transport capacity in laminar interrill flow on stone covered surfaces. Water Resour. Res. 35, 305-310.

Li, G., Abrahams, A.D., Atkinson, J.F., 1996. Correction factors in the determination of mean velocity of overland flow. Earth Surf. Process. Landf. 21(6), 509-515.

Li, Y.H., Xie, L., Su, T.C., 2018. Resistance of open-channel flow under the effect of bending deformation of submerged flexible vegetation. J. Hydraul. Eng. 144(3), 04017072.

Mahmoodabadi, M., Ghadiri, H., Rose, C., Yu, B., Rafahi, H., Rouhipour, H., 2014. Evaluation of GUEST and WEPP with a new approach for the determination of sediment transport capacity. J. Hydrol. 513, 413-421.

Mu, H.L., Yu, X.J., Fu, S.H., Yu, B.F., Liu, Y.N., Zhang, G.H., 2019. Effect of stem basal cover on the sediment transport capacity of overland flows. Geoderma, 337: 384-393.

Pan, C.Z., Ma, L., Shangguan, Z.P., 2010. Effectiveness of grass strips in trapping suspended sediments from runoff. Earth Surf. Process. Landf. 35(9), 1006-1013.

Pan, C.Z., Shangguan, Z.P., 2006. Runoff hydraulic characteristics and sediment generation in sloped grassplots under simulated rainfall conditions. J. Hydrol. 331(1), 178-185.

Roels, J.M., 1984. Flow resistance in concentrated overland flow on rough slope surfaces. Earth Surf. Process. Landf. 9(6), 541-551.

Rogers, R.D., Schumm, S.A., 1991. The effect of sparse vegetative cover on erosion and sediment yield. J. Hydrol. 123, 19-24.

Salman, M., Manochehr, G., Ali, J., 2012. Effect of rock fragments cover on distance of rill erosion initiation and overland flow hydraulics. Int. J. Soil Sci. 7(3), 100-107.

SCS, 1954. Handbook of channel design for soil and water conservation, Soil Conservation Service SCS-TP-61. USDA, Washington, DC.

Shi, H., Shao, M., 2000. Soil and water loss from the Loess Plateau in China. J. Arid Environ. 45(1), 9-20.

Sun, W., Shao, Q., Liu, J., 2013. Soil erosion and its response to the changes of precipitation and vegetation cover on the Loess Plateau. J. Geogr. Sci. 23(6), 1091-1106.

Termini, D., 2009. Experimental observations of flow and bed processes in large-amplitude meandering flume. J. Hydraul. Eng. 135(7): 575-587.

Termini, D., 2015. Momentum transport and bed shear stress distribution in a meandering bend: experimental analysis in a laboratory flume. Adv. Water Resour. 81: 128-141.

Termini, D., 2016. Experimental analysis of the effect of vegetation on flow and bed shear stress distribution in high-curvature bends. Geomorphology 274: 1-10.

Termini, D., Piraino, M., 2011. Experimental analysis of cross-sectional flow motion in a large amplitude meandering bend. Earth Surf. Process. Landf. 36(2): 244-256.

Turner, A.K., Chanmeesri, N., 1984. Shallow flow of water through non-submerged vegetation. Agr. Water Manage. 8(4), 375-385.

Wainwright, J., 2000. Plot scale studies of vegetation, overland flow and erosion interactions: case studies from Arizona and New Mexico. Hydrol. process. 14(16-17), 2921-2943.

White, B.L., Nepf, H.M., 2008. A vortex based model of velocity and shear stress in a partially vegetated shallow channel. Water Resour. Res. 44, W01412.

Wilson, C., 2007. Flow resistance models for flexible submerged vegetation. J. Hydrol. 342(3), 213-222.

Wu, S.F., Wu, P.T., Feng, H., Merkley, G.P., 2011. Effects of alfalfa coverage on runoff, erosion and hydraulic characteristics of overland flow on loess slope plots. Front. Environ. Sci. Eng. 5(1), 76-83.

Wu, W.M., He, Z.G., 2009. Effects of vegetation on flow conveyance and sediment transport capacity. Int. J. Sediment Res. 24(3): 247-259.

Yalin, M.S., 1963. An expression for bed-load transportation. J. Hydraul. Div. 89, 221-250.

Yang, C.T., 1972. Unit stream power and sediment transport. J. Hydraul. Div. 98, 1805-1826.

Zhang, G., Liu, G., Wang, G., Wang, Y., 2012. Effects of patterned artemisia capillaris on overland flow velocity under simulated rainfall. Hydrol. process. 26(24), 3779-3787.

Zhang, G.H., Liu, Y.M., Han, Y.F., Zhang, X.C., 2009. Sediment transport and soil detachment on steep slopes: I. Transport capacity estimation. Soil Sci. Soc. Am. J. 73(4): 1291-1297.

Zhang, G.H., Luo, R.T., Cao, Y., Shen, R.C., Zhang, X.C., 2010. Correction factor to dye-measured flow velocity under varying water and sediment discharges. J. Hydrol. 389(1), 205-213.

Zhang, G.H., Wang, L.L., Tang, K.M., Luo, R.T., Zhang, X.C., 2011. Effects of sediment size on transport capacity of overland flow on steep slopes. Hydrol. Sci. J. 56(7), 1289-1299.

Zhang, J., Zhong, Y., Huai, W., 2018. Transverse distribution of streamwise velocity in open-channel flow with artificial emergent vegetation. Ecol. Eng. 110, 78-86.

Zhang, K., Wang, Z., Wang, G., Sun, X., Cui, N., 2017. Overland-flow resistance characteristics of nonsubmerged vegetation. J. Irrig. Drain. Eng. 143(8), 04017021.

Zhao, C.H., Gao, J.E., Huang, Y.F., Wang, G.Q., Zhang, M.J., 2016. Effects of vegetation stems on hydraulics of overland flow under varying water discharges. Land Degrad. Dev. 27(3), 748-757.

Zhao, X., Wu, P., Gao, X., Persaud, N., 2015. Soil quality indicators in relation to land use and topography in a small catchment on the Loess Plateau of China. Land Degrad. Dev. 26(1), 54-61.

Zhou, Z.C., Shangguan, Z.P., 2008. Effect of ryegrasses on soil runoff and sediment control. Pedosphere 18(1), 131-136.

Zhu, X.M., 1984. The main types and related factors of water erosion on the loess plateau. Bull. Soil Water Conserv. 4, 40-44.

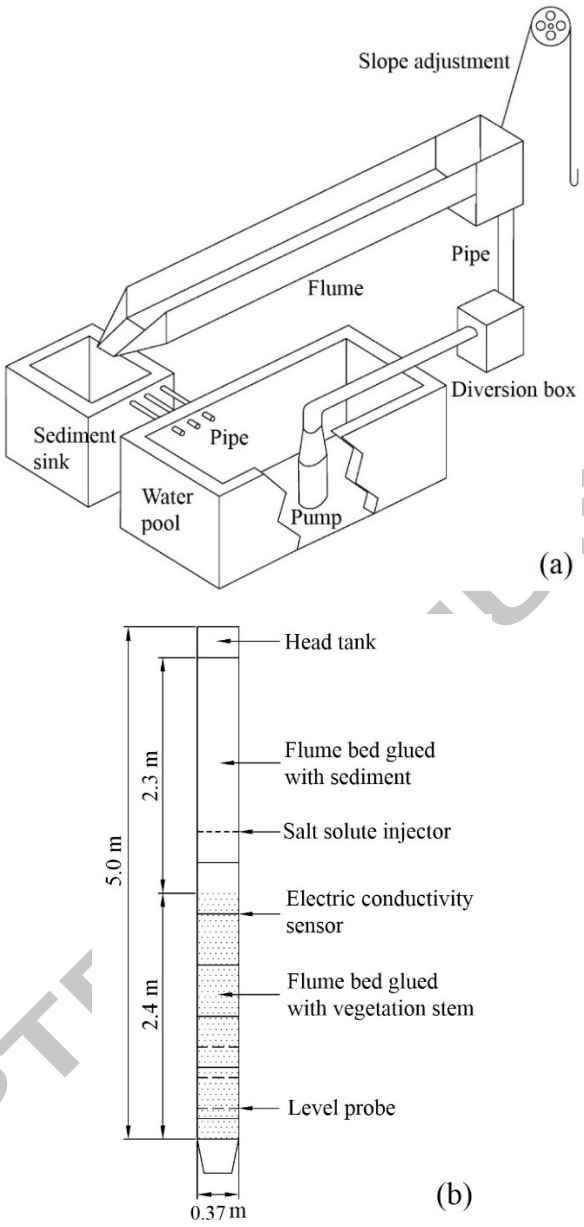

Figure 1. Experimental setup to measure the hydraulic parameters.

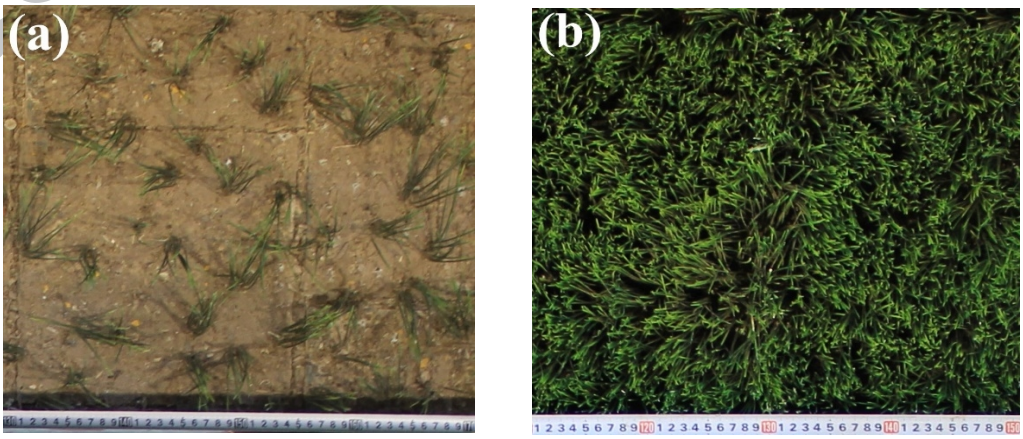

Figure 2. Arial view of the artificial Gramineae stem cover. (a): *C*=1.25%, (b): *C*=30%.

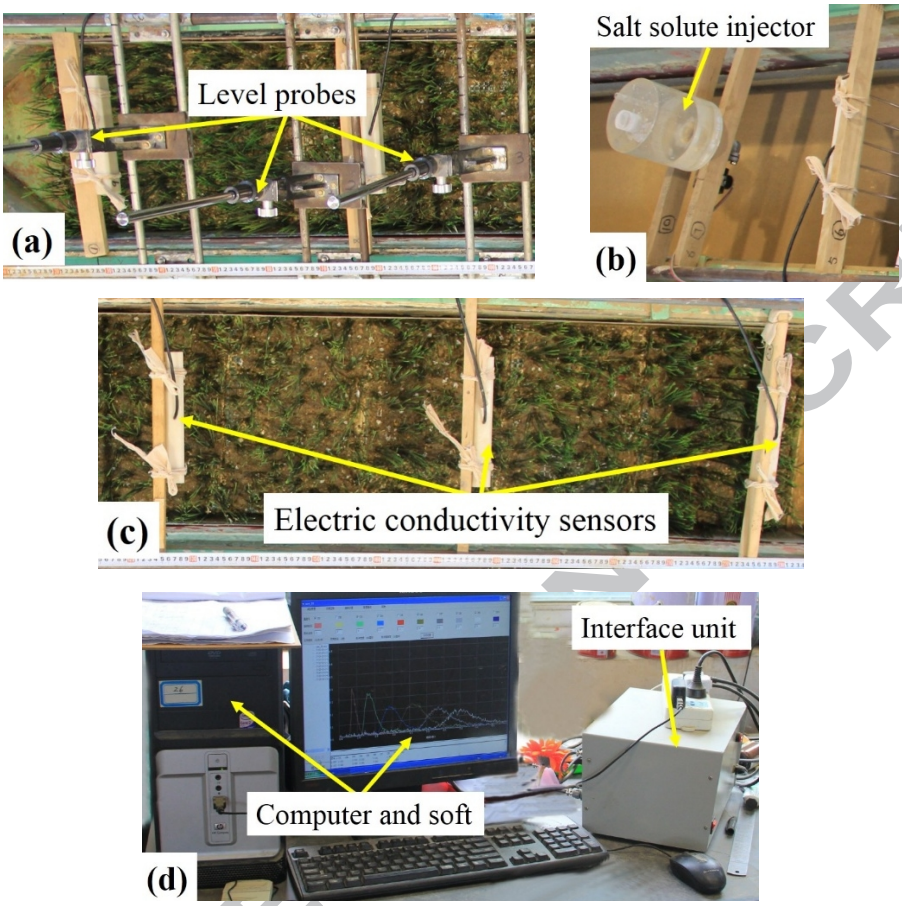

Figure 3. Experimental equipment to measure velocity and flow depth.

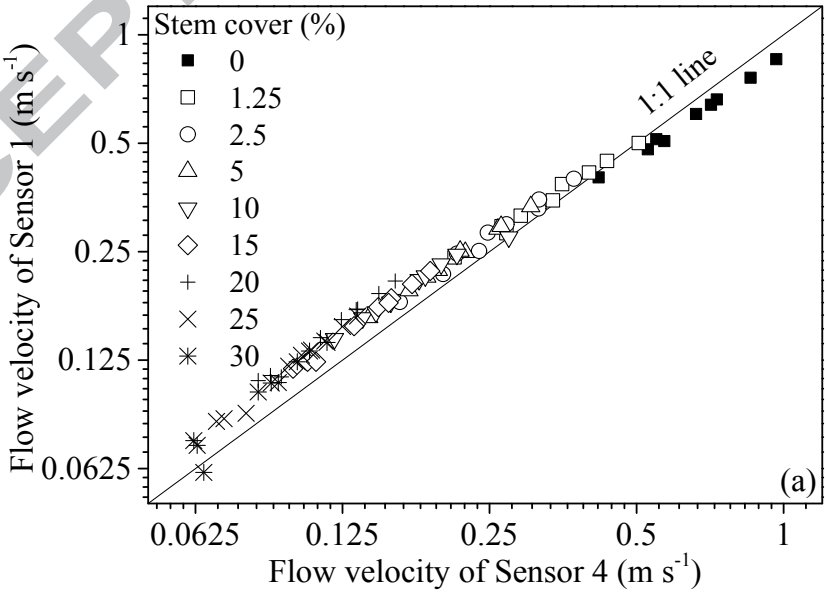

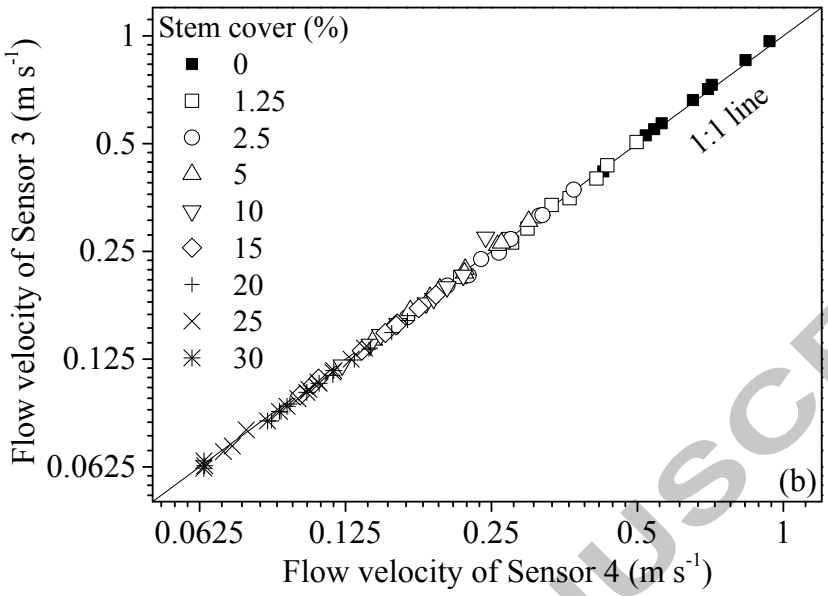

Figure 4. The relationship among velocity measurements at different locations for different levels of stem cover. Sensors 1, 3, and 4 were located at 1.7 m, 0.7 m, and 0.2 m, respectively, upstream from the end of the flume.

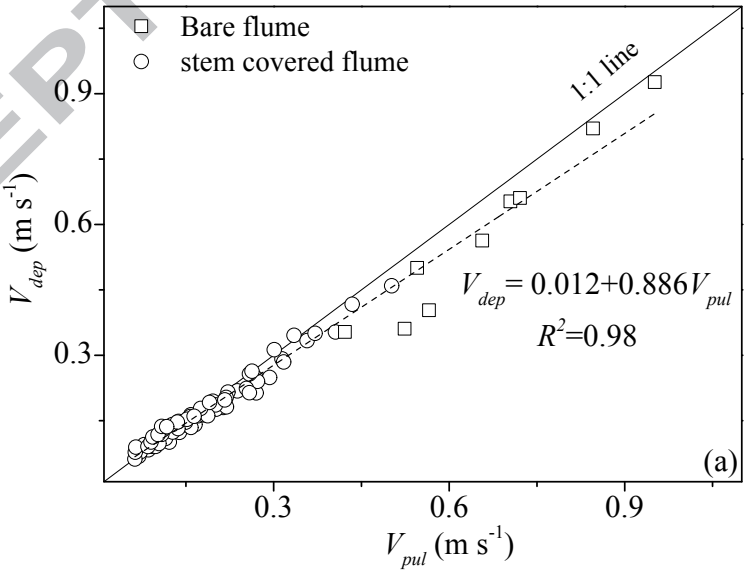

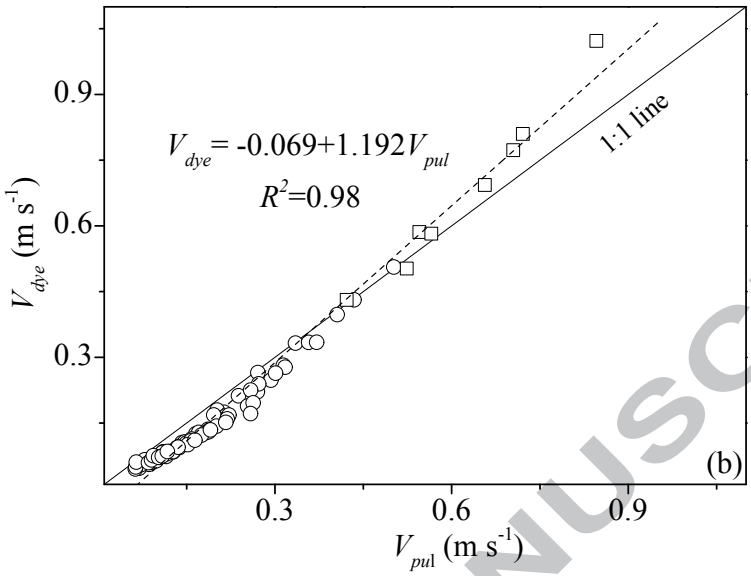

Figure 5. Comparison of the mean velocities using different measurement methods. V_{pul} was the mean velocity measured with the electrolyte pulse method; V_{dye} was the mean velocity measured with the $KMnO_4$ tracing method; and V_{dep} was determined with the continuity equation and measured flow depth.

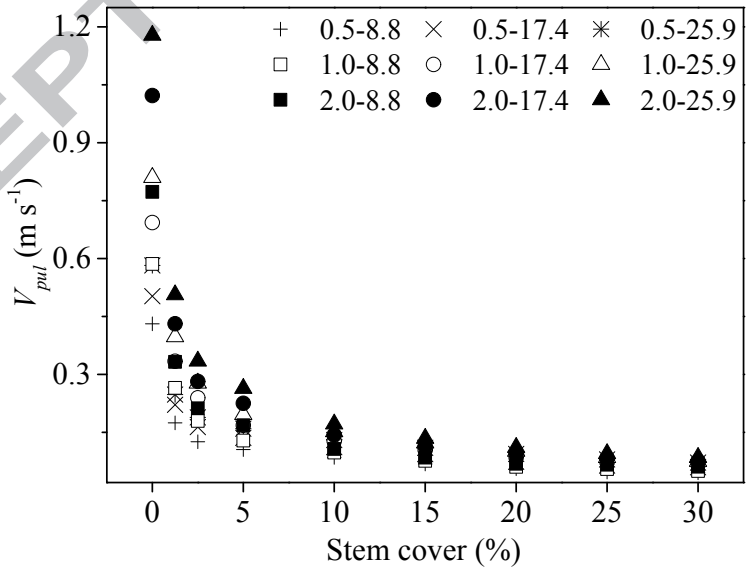

Figure 6. Flow velocity (V_{pul}) for different combinations of stem cover, discharge and slope gradient. Discharge range: 0.5, 1.0, 2.0×10^{-3} m^3 s^{-1} and slope gradient range: 8.8, 17.4, 25.9%.

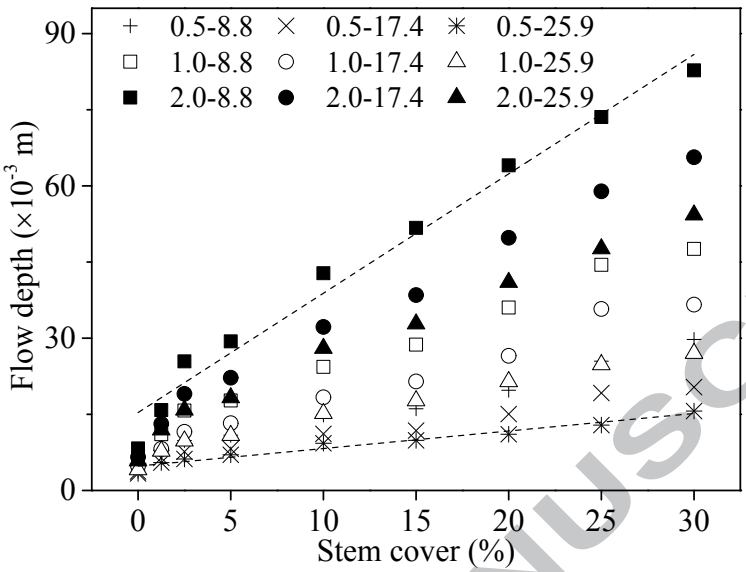

Figure 7. Flow depth (*H*) for different combinations of stem cover, discharge and slope gradient. Discharge range: 0.5, 1.0, 2.0×10^{-3} m^3 s^{-1}; slope gradient range: 8.8, 17.4, 25.9%.

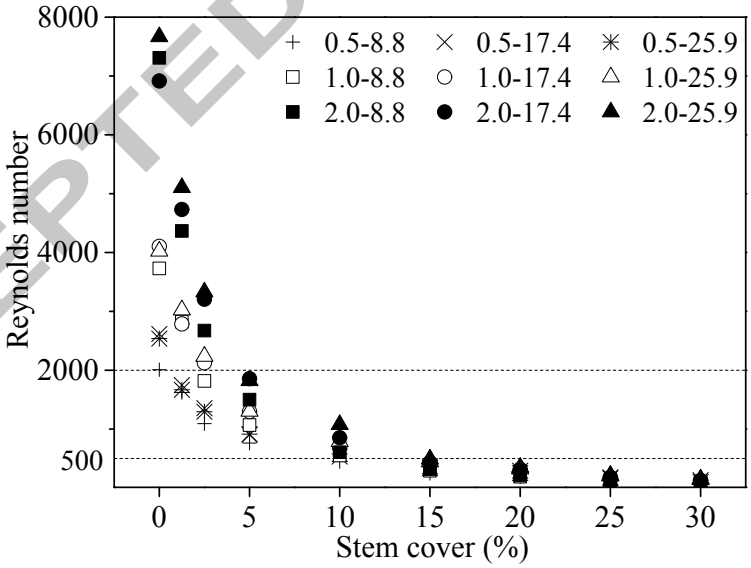

Figure 8. Reynolds number (*Re*) for different combinations of stem cover, discharge and slope gradient. Discharge range: 0.5, 1.0, 2.0×10^{-3} m^3 s^{-1}; slope gradient range: 8.8, 17.4, 25.9%.

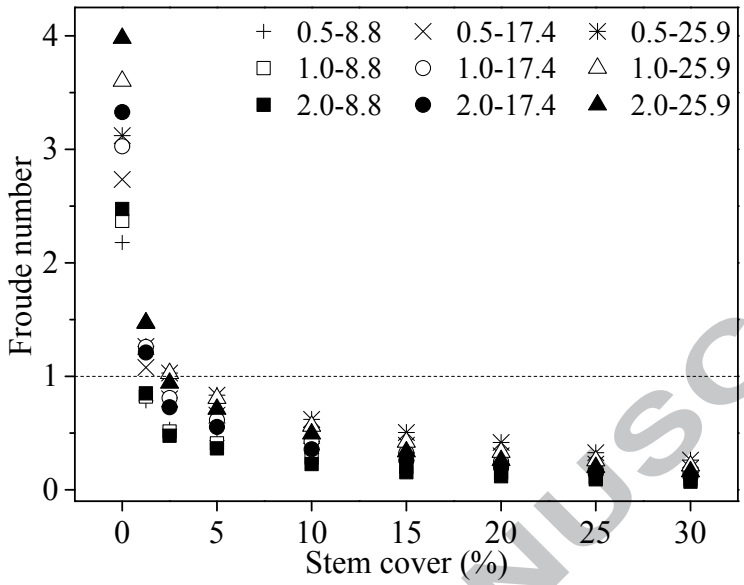

Figure 9. Froude number (*Fr*) for different combinations of stem cover, discharge and slope gradient. Discharge range: 0.5, 1.0, 2.0×10^{-3} m^3 s^{-1}; slope gradient range: 8.8, 17.4, 25.9%.

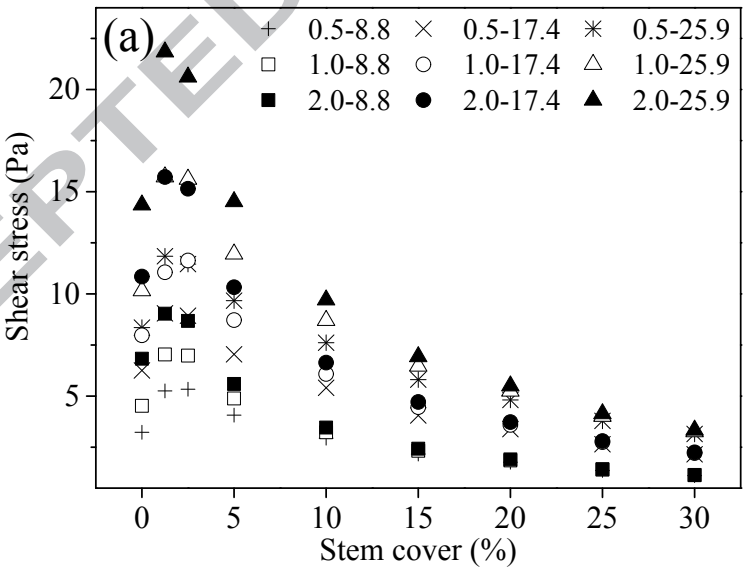

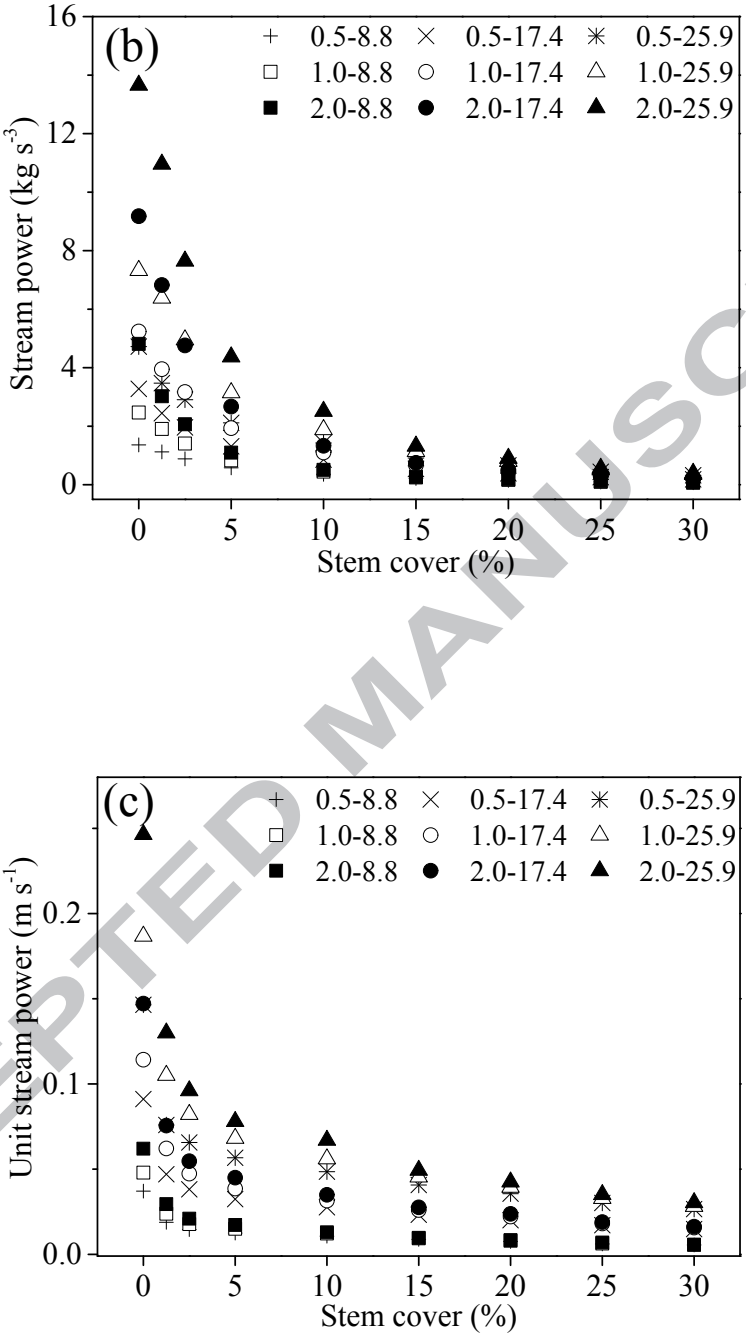

Figure 10. Shear stress, τ, (a); stream power, Ω, (b); and unit stream power, ω, (c) as functions of the stem cover for different combinations of discharge and slope gradient. Discharge range: 0.5, 1.0, 2.0×10^{-3} m^3 s^{-1}; slope gradient range: 8.8, 17.4, 25.9%.

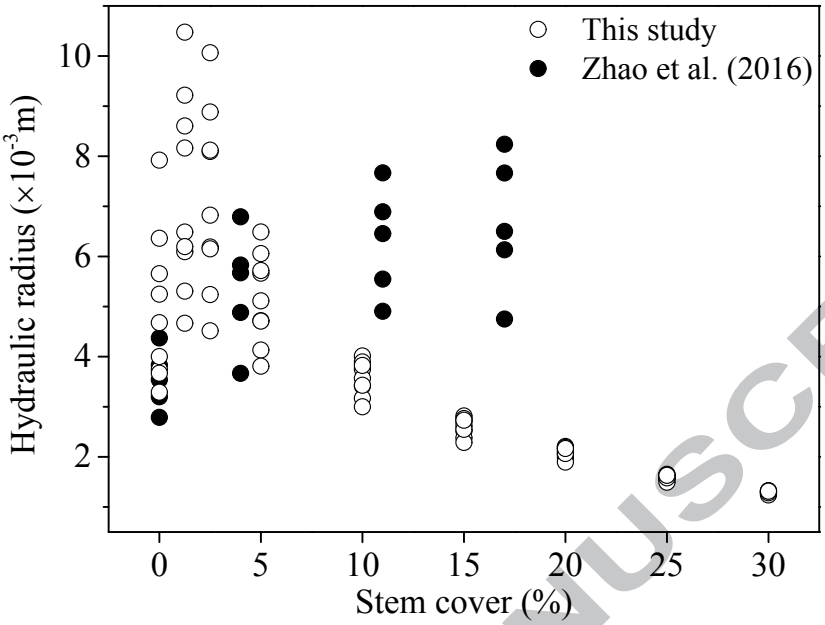

Figure 11. Comparison of the hydraulic radius for different level of stem covers between this study and Zhao et al. (2016).

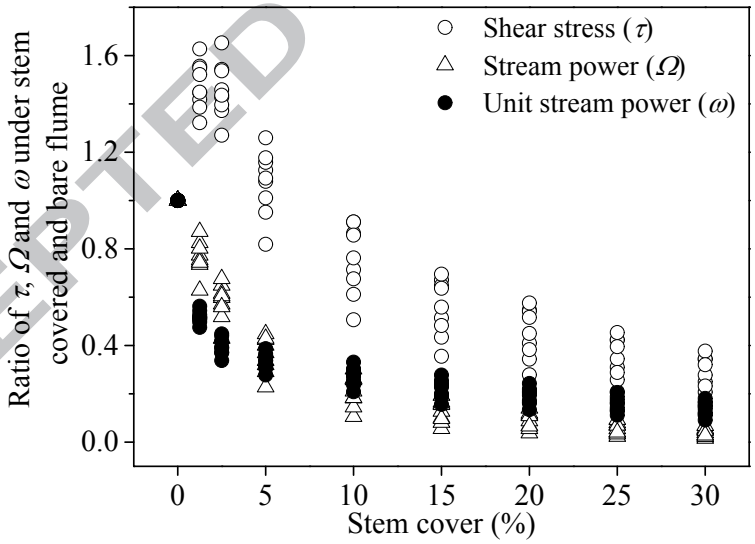

Figure 12. Relationship between stem cover and shear stress (τ), stream power (Ω) and unit stream power (ω) relative to those without stem cover.

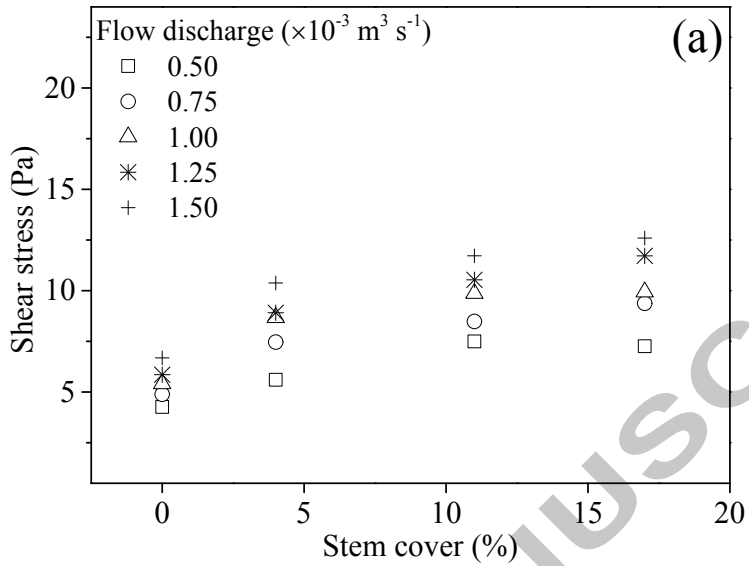

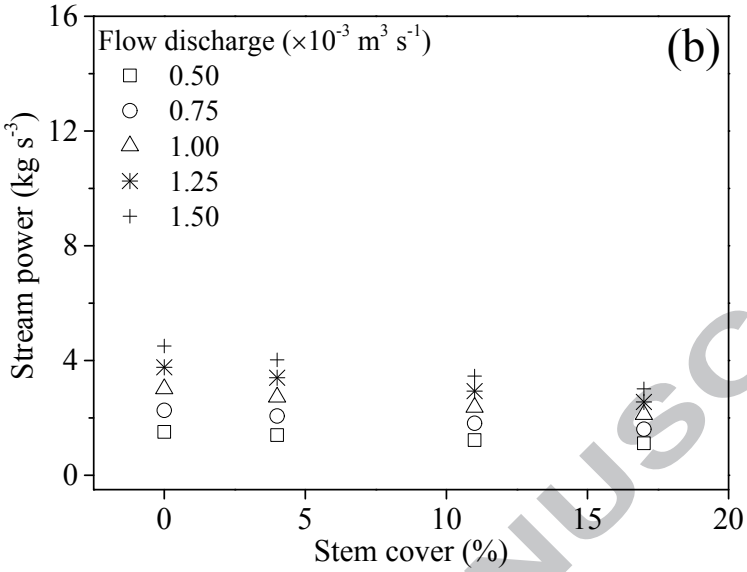

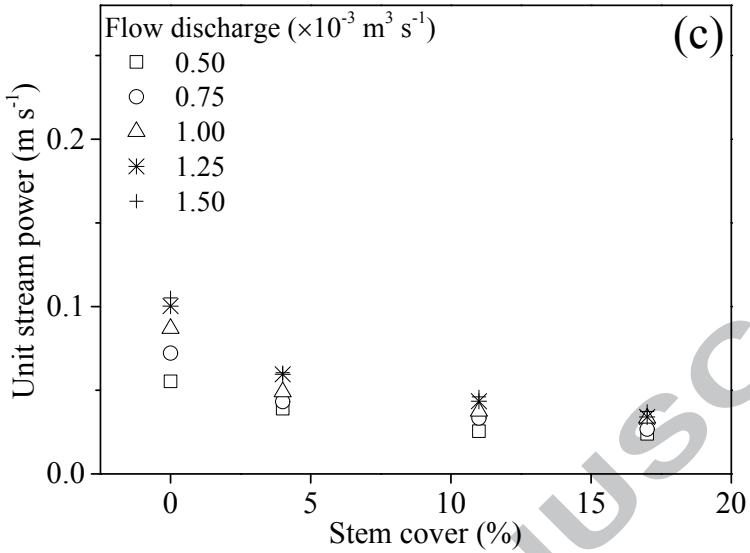

Figure 13. Relationship between stem cover and (a) shear stress, τ, (b) stream power, Ω, (c) unit stream power, ω for different discharge ranging from 0.5 to 1.5 $\times 10^{-3}$ $m^3 s^{-1}$ (Zhao et al., 2016). The slope gradient is fixed at 15.6% (Zhao et al., 2016)

Table 1. Measured flow velocity (m s^{-1}) at four longitudinal sections with the electrolyte pulse method for 81 combinations of stem cover, discharge and slope gradient.

Sensor number	Distance from the end of flume (m)	Slope gradient (%)	Flow discharge (10^{-3} m^3 s^{-1})	Stem cover (%)								
				0	1.25	2.5	5	10	15	20	25	30
1	2.2-1.7	8.8	0.5	0.402	0.241	0.181	0.164	0.143	0.118	0.110	0.085	0.075
			1	0.513	0.281	0.217	0.195	0.164	0.124	0.113	0.086	0.073
			2	0.640	0.347	0.251	0.222	0.170	0.124	0.112	0.089	0.061
		17.4	0.5	0.481	0.294	0.247	0.213	0.181	0.155	0.144	0.120	0.102
			1	0.603	0.385	0.298	0.249	0.209	0.176	0.162	0.129	0.108
			2	0.760	0.447	0.330	0.289	0.231	0.186	0.173	0.133	0.108
		25.9	0.5	0.507	0.315	0.283	0.251	0.214	0.180	0.173	0.141	0.124
			1	0.662	0.415	0.349	0.294	0.246	0.203	0.191	0.155	0.133
			2	0.856	0.501	0.399	0.334	0.275	0.221	0.207	0.166	0.140
2	1.7-1.2	8.8	0.5	0.423	0.228	0.174	0.149	0.132	0.107	0.095	0.075	0.067
			1	0.530	0.281	0.210	0.175	0.151	0.112	0.099	0.077	0.067
			2	0.672	0.343	0.245	0.201	0.158	0.113	0.101	0.083	0.063
		17.4	0.5	0.504	0.291	0.234	0.193	0.168	0.142	0.128	0.107	0.091
			1	0.627	0.370	0.286	0.227	0.196	0.158	0.141	0.114	0.096
			2	0.794	0.447	0.324	0.266	0.217	0.168	0.151	0.118	0.098
		25.9	0.5	0.540	0.307	0.270	0.228	0.200	0.165	0.152	0.126	0.110
			1	0.697	0.423	0.332	0.269	0.230	0.185	0.168	0.138	0.117
			2	0.901	0.508	0.383	0.309	0.256	0.201	0.182	0.148	0.124
3	1.2-0.7	8.8	0.5	0.425	0.216	0.168	0.143	0.123	0.101	0.088	0.070	0.064
			1	0.542	0.271	0.203	0.170	0.141	0.107	0.092	0.073	0.064
			2	0.699	0.333	0.238	0.196	0.148	0.110	0.096	0.078	0.064
		17.4	0.5	0.520	0.276	0.224	0.187	0.160	0.135	0.118	0.100	0.086
			1	0.651	0.362	0.274	0.221	0.183	0.151	0.130	0.105	0.091
			2	0.836	0.433	0.314	0.257	0.203	0.160	0.140	0.110	0.095
		25.9	0.5	0.561	0.297	0.259	0.220	0.190	0.159	0.141	0.118	0.104
			1	0.712	0.412	0.319	0.262	0.219	0.177	0.156	0.128	0.110
			2	0.936	0.498	0.370	0.298	0.243	0.192	0.168	0.137	0.118
4	0.7-0.2	8.8	0.5	0.418	0.212	0.164	0.142	0.120	0.099	0.084	0.069	0.062
			1	0.549	0.271	0.201	0.171	0.138	0.106	0.089	0.072	0.063
			2	0.710	0.337	0.238	0.196	0.146	0.110	0.094	0.079	0.065
		17.4	0.5	0.527	0.265	0.215	0.186	0.157	0.132	0.113	0.097	0.084
			1	0.662	0.352	0.271	0.223	0.179	0.148	0.124	0.103	0.089
			2	0.856	0.435	0.315	0.260	0.199	0.157	0.133	0.108	0.092
		25.9	0.5	0.570	0.290	0.248	0.218	0.185	0.155	0.134	0.115	0.101
			1	0.730	0.400	0.316	0.264	0.214	0.174	0.148	0.125	0.107
			2	0.966	0.505	0.372	0.304	0.274	0.189	0.160	0.134	0.116

Table 2. The mean flow velocity (V_{pul} and V_{dye}) with the electrolyte pulse and $KMnO_4$ tracing method for 81 combinations of stem cover, discharge and slope gradient.

	Slope gradient (%)	Flow discharge (10^{-3} m^3 s^{-1})	Stem cover (%)								
			0	1.25	2.5	5	10	15	20	25	30
V_{pul} (m s^{-1})	8.8	0.5	0.422	0.214	0.166	0.142	0.122	0.100	0.086	0.070	0.063
		1	0.524	0.270	0.219	0.186	0.159	0.134	0.115	0.098	0.085
		2	0.566	0.293	0.254	0.219	0.187	0.157	0.138	0.116	0.103
	17.4	0.5	0.545	0.271	0.202	0.171	0.139	0.107	0.091	0.072	0.064
		1	0.656	0.357	0.272	0.222	0.181	0.150	0.127	0.104	0.090
		2	0.721	0.406	0.317	0.263	0.217	0.175	0.152	0.127	0.109
	25.9	0.5	0.705	0.335	0.238	0.196	0.147	0.110	0.095	0.079	0.064
		1	0.846	0.434	0.314	0.259	0.201	0.159	0.137	0.109	0.094
		2	0.951	0.502	0.371	0.301	0.259	0.191	0.164	0.136	0.117
V_{dye} (m s^{-1})	8.8	0.5	0.431±0.074	0.174±0.014	0.126±0.008	0.105±0.004	0.085±0.002	0.068±0.003	0.056±0.002	0.047±0.002	0.045±0.006
		1	0.586±0.031	0.265±0.013	0.180±0.009	0.129±0.004	0.098±0.003	0.076±0.002	0.061±0.002	0.055±0.006	0.050±0.009
		2	0.773±0.041	0.332±0.013	0.212±0.011	0.168±0.003	0.107±0.004	0.085±0.004	0.069±0.006	0.066±0.010	0.061±0.011
	17.4	0.5	0.503±0.055	0.221±0.017	0.164±0.016	0.136±0.008	0.112±0.004	0.094±0.003	0.074±0.003	0.064±0.003	0.060±0.007
		1	0.693±0.067	0.334±0.021	0.239±0.019	0.168±0.008	0.127±0.003	0.104±0.004	0.084±0.002	0.072±0.006	0.066±0.010
		2	1.022±0.097	0.431±0.024	0.282±0.015	0.225±0.006	0.143±0.003	0.113±0.003	0.095±0.004	0.083±0.012	0.076±0.015
	25.9	0.5	0.582±0.072	0.248±0.023	0.189±0.019	0.159±0.009	0.130±0.004	0.110±0.005	0.094±0.003	0.080±0.005	0.072±0.008
		1	0.810±0.089	0.397±0.031	0.277±0.021	0.196±0.010	0.151±0.005	0.122±0.003	0.101±0.002	0.085±0.006	0.075±0.008
		2	1.178±0.117	0.506±0.043	0.334±0.018	0.264±0.007	0.172±0.004	0.134±0.004	0.111±0.003	0.095±0.013	0.085±0.012

Table 3. Compare of the measured velocities for different methods.

Statistical parameter	Compared to V_{dep}		Compared to V_{dye}	
	V_{pul}	V_{dye}	V_{pul}	V_{dep}
MAE (kg s^{-1}m^{-1})	0.022	0.045	0.041	0.045
RRMSE	0.164	0.285	0.244	0.297
NSE	0.951	0.853	0.945	0.918

Note: V_{pul} was the mean velocity measured with the electrolyte pulse method; V_{dye} was the mean velocity measured with the $KMnO_4$ tracing method; and V_{dep} was determined with the continuity equation and measured flow depth.

Table 4. The range of the reduction factor for flow velocity, flow depth, shear stress, stream power, and unit stream power for different levels of stem cover. The variation in the reduction factor occurred as a result of different combinations of slope gradient and discharge.

Stem cover (%)	1.25	2.5	5	10	15	20	25	30
Flow velocity	0.48-0.56	0.34-0.45	0.28-0.39	0.21-0.33	0.16-0.28	0.13-0.24	0.11-0.21	0.09-0.18
Flow depth	1.64-2.05	1.85-3.07	2.10-3.55	2.77-5.17	2.95-6.25	3.31-7.74	3.85-8.94	4.67-10.00
Shear stress	1.32-1.63	1.27-1.65	0.82-1.26	0.51-0.91	0.36-0.70	0.28-0.58	0.21-0.45	0.17-0.38
Stream power	0.63-0.87	0.43-0.68	0.23-0.45	0.11-0.30	0.06-0.19	0.04-0.14	0.02-0.09	0.02-0.07
Unit stream power	0.48-0.56	0.34-0.45	0.28-0.39	0.21-0.33	0.16-0.28	0.13-0.24	0.11-0.21	0.09-0.18

Table 5. Equations for shear stress, stream power and unit stream power without and with stem cover.

Equation number	Equation of bare and stem covered flume	*NSE*	R^2
16	$\tau_0 = 352.565S^{0.728}q^{0.425}$	0.99	0.99
17	$\Omega_0 = 2659.792S^{1.089}q^{0.736}$	0.99	0.99
18	$\omega_0 = 9.036S^{1.266}q^{0.367}$	0.99	0.99
19	$\tau = \tau_0 \exp(-0.035C)$	0.73	0.84
20	$\Omega = \Omega_0 \exp(-0.179C)$	0.98	0.98
21	$\omega = \omega_0 \exp(-0.150C)$	0.71	0.84

Note: shear stress (Pa), τ; stream power (kg s^{-3}), Ω; unit stream power (m s^{-1}), ω; slope (m m^{-1}), S; unit flow discharge (m^2 s^{-1}), q; stem cover (%), C.

Table 6. Performance of various empirical equations for shear stress, stream power and unit stream power under independent variables of slope and discharge without and with stem cover.

References	Experiment condition	Experiment material	Slope (m m^{-1})	Unit discharge (10^{-3} m^2 s^{-1})	Equation number	*RRMSE*	*NSE*	R^2
Zhang et al., (2011)	Non-eroding bed /overland flow	Sand	8.8-46.6	0.66-5.26	16	0.31	0.50	0.99
					17	0.14	0.96	0.98
					18	0.18	0.90	0.98
Pan and Shangguan, (2006)	Eroding bed /simulated rainfall;	Soil	25.9;	0.032-0.04;	19	0.92	-17.42	0.95
					20	1.55	-320.18	0.96
					21	1.68	-18.24	0.96
Zhao et al., (2016)	Non-eroding bed /overland flow	Soil	15.6	1.0-3.0	19	0.55	-2.69	0.07
					20	0.60	-1.65	0.39
					21	0.33	0.48	0.90

Highlights:

- We measured flow depth and velocity with different vegetation stem cover, slope gradient and flow discharge.
- The reduction in flow velocity can be as high as 90% for 30% stem cover based on this set of experiments.
- The shear stress, stream power and unit stream power were all significantly affected by the stem cover and slope.
- The shear stress, stream power and unit stream power could all broadly be described with an exponential delay function of the cover.